IDRiM (2024) 14 (2) ISSN: 2185-8322
DOI10.5595/001c.123359

Journal of Integrated Disaster Risk Management

Regular Article

Assessing Tropical Cyclone Destruction Using Landsat Satellite Imagery: a Case Study in Bangladesh

Abdullah Salman[1*], Ayon Saha[1], Saleh Shakeel Nomaan[2], Emdadul Haque[1] and Tajim Asadi[3]

Received: 24/10/2023 / Accepted: 10/04/2024 / Published online: 06/09/2024

Abstract Tropical cyclones are extreme natural catastrophes and are anticipated to intensify strength and recurrence under upcoming climate change consequences in our coastal regions through Bangladesh. This study has tested and developed methods for evaluating considerable damages affected in 2020 by cyclone Amphan in Satkhira district (3817.29 km^2) in Bangladesh from 30m spatial-resolution satellite imageries. Iso-cluster unsupervised classification procedures are applied to prepare maps in pre- and post-cyclone Landsat 8 imagery. A difference between the pre- and post-cyclone image classification and NDVI analysis give us evidence about the significant landscape changes at the Cyclone Amphan impact on the study area. The total accuracies for pre- and post-cyclone images classification were 70% and 68% respectively. The outcomes indicate that 35.09% of the study region was remarkably influenced by cyclone Amphan. Statistical analysis indicates that water bodies have dramatically increased 17.65% in different land cover areas due to the strong water surge. On the contrary, the classified image showed that the vegetation and agricultural land decreased 4.13% and 10.82%. Thus, land covers have inundated due to heavy flash during the cyclone. Barren land also decreased 1.80%, and low land areas were also flooded 0.36% due to heavy water flashes. NDVI analysis indicated no destruction of any vegetation species, but vegetation damage is considerable. The developed method may be imposed in future to measure the impacts produced by cyclones in Bangladesh and to make policies for the commitments of cyclone disaster controlling and management.

Keywords: Coastal area, Cyclone Amphan, NDVI, Satkhira, Storm water

[1] Geology and Mining, University of Barisal, Bangladesh
[2] Applied Geoinformatics, Paris Lodron University, Austria
[3] Accounting and Information Systems, University of Barisal, Bangladesh
* Corresponding author email: masalman@bu.ac.bd

1. INTRODUCTION

Cyclones are one of the most significant catastrophic events that ordinarily generate storm floods and concentrated precipitation with high winds (Hoque et al., 2016). Significant numbers of the world coastal areas are highly prone to cyclones and related storm surges (Salman et al., 2018; Klemas, 2009). These disasters cause significant loss of life, assets and environmental damage in large-scale, and are more likely to increase intensity and recurrence due to a warming climate (Salman, 2022; Knutson et al., 2010). Most of the landscapes are troubled and damaged by tropical cyclones in the affected regions. The occurrence of the cyclone has increased over the world due to changes in the climatic variables and humans interventions in natural streams (Salman & Ahmed, 2020; Henderson-Sellers et al., 1998). Remote sensing technology can be a cost-effective, accurate, and prospective tool for mapping the damages of tropical cyclones from small to large areas with supervision approaches (Vatsavai et al., 2011). Advanced remote sensing techniques permit us to use low (> 100 m pixels) to high (< 5 m pixels) resolution multispectral and panchromatic satellite images of the same areas pre- and post-tropical cyclone catastrophe for mapping the affected and damaged landscapes.

The geographic position of Bangladesh and the funnel-shaped Bay of Bengal intensify devastating tropical cyclones (Salman, 2022; Das, 1972). Tropical cyclones predominantly affect the lives and properties in low-lying coastal areas. Cyclone-induced storm surges in this area typically initiate in the central and southern parts of the Bay of Bengal or in the Andaman Sea. Due to the shallow continental shelf, the surge amplifies significantly as it is headed for land and causes catastrophic floods along the coast (Murty et al., 1986). In the northern Bay of Bengal, a unique combination of high tides, a funneling coastal configuration, the low flat coastal terrain and a high population density have originated some of the highest mortality figures associated with storm surges (Flierl & Robinson, 1972). However, Bangladesh is one of the most vulnerable countries due to global climate change and sea-level rise. The country is likely to be affected by more powerful cyclonic events in the anticipatable future. The consequences of climate change lead to an increase in the cyclone-prone area and put many people at risk.

During the years 1797 to 2020, Bangladesh has been hit by around 85 severe cyclones, 40 of which were accompanied by storm surges. A tropical cyclone occurring in the Bay of Bengal incorporates a lifetime of one week or longer. The height of the surges is constrained to a maximum of 10 meters in the bay. When propagating into the shallower inland and coastal areas, the heights of these waves are further condensed. The wave's frequency (surge plus tide) with a height of about 7-8 m is approximately once per 20 years. A storm surge of approximately once in 5 years has a height of about 4-5 m (surge plus tide). Besides these surges, wind waves occur, which depend on wind speed and direction, fetch, water depth and duration. The waves about 3-5 m height may occur under unfavorable conditions in the coastal regions (French Engineering Consortium and Bangladesh Water Development Board 1989).

Cyclone Amphan, which occurred in May 2020, caused massive damage in several parts of the country. Along the coastline of Bangladesh, the 'extremely severe cyclonic storm' caused extensive damage as extreme winds, heavy rainfall, thunder, and lightning are reported.

The aim of this study approaches for mapping multiple types of damage such as vegetation destruction, vegetation defoliation, destruction of infrastructure, damage to infrastructure, change to landforms caused in 2020 by tropical Cyclone Amphan in Satkhira district (3817.29 km^2) of Bangladesh using unsupervised classification from moderate spatial resolution satellite imagery.

2. METHODS AND MATERIALS

2.1 Study Area, Cyclone Amphan & Data Sets

Satkhira is a district with approximately 3817.29 km^2 area in the southwestern part of Bangladesh. It border by the Jessore district to the north and by the Bay of Bengal on the south. The study region is located within the 21036' and 22054' north latitudes and in-between 88054' and 89020' east longitudes (Figure 1). Satkhira district, a part of Khulna division, is consists of seven Upazilas (small administrative unit) called Satkhira Sadar, Assasuni, Kalaroa, Debhata, Kaliganj, Tala, Shyamnagar and Kalaroa Upazila. The study area is situated more or less than 1m above sea level and is flat (Didar-Ul Islam et al., 2015). Due to the geographic position and the adjacent Bay of Bengal, tropical cyclones severely affected this area.

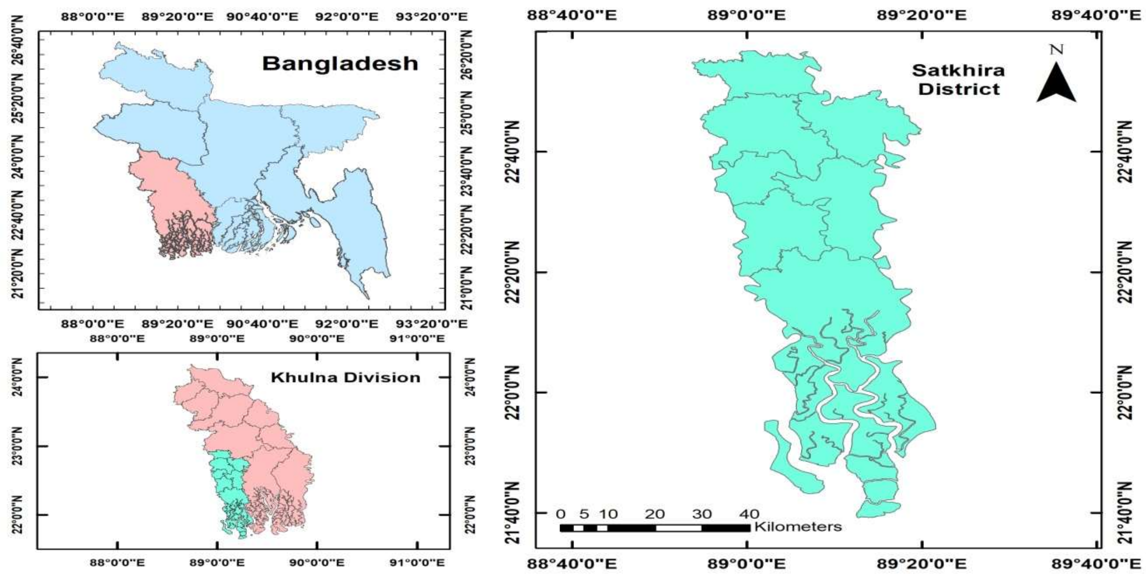

Figure 1. Location of the study area, Satkhira district with Sundarbans Mangrove Forest with river distributions in the southern portion under Khulna Division in Bangladesh.

Cyclone Amphan, a category 5 tropical cyclone, struck the southwestern part of Bangladesh, specially Satkhira District and India, with a typical speed of 260 km/h on May 16, 2020, and dissipated on May 21, 2020 (Balasubramanian & Chalamalla, 2020) (Figure 2). It was one of the supreme potent cyclones in the last twenty years, recently hit Bangladesh and destroyed communities and millions of residents. Over a million people were affected by Amphan cyclone across several districts of Khulna and Barishal. About 26 individuals lost their lives and added damages assessed at approximately US$ 130 million by this cyclone. LANDSAT-8 OLI-TIRS images acquired on May 08, 2020, before the tropical cyclone Amphan, and June 09, 2020, after the cyclone, were applied in this study (Figure 3). Both images were at 30m spatial resolution. The images were used for unsupervised image classification to determine the change detection after the cyclone. Detailed information on the satellite imageries is presented in Table 1.

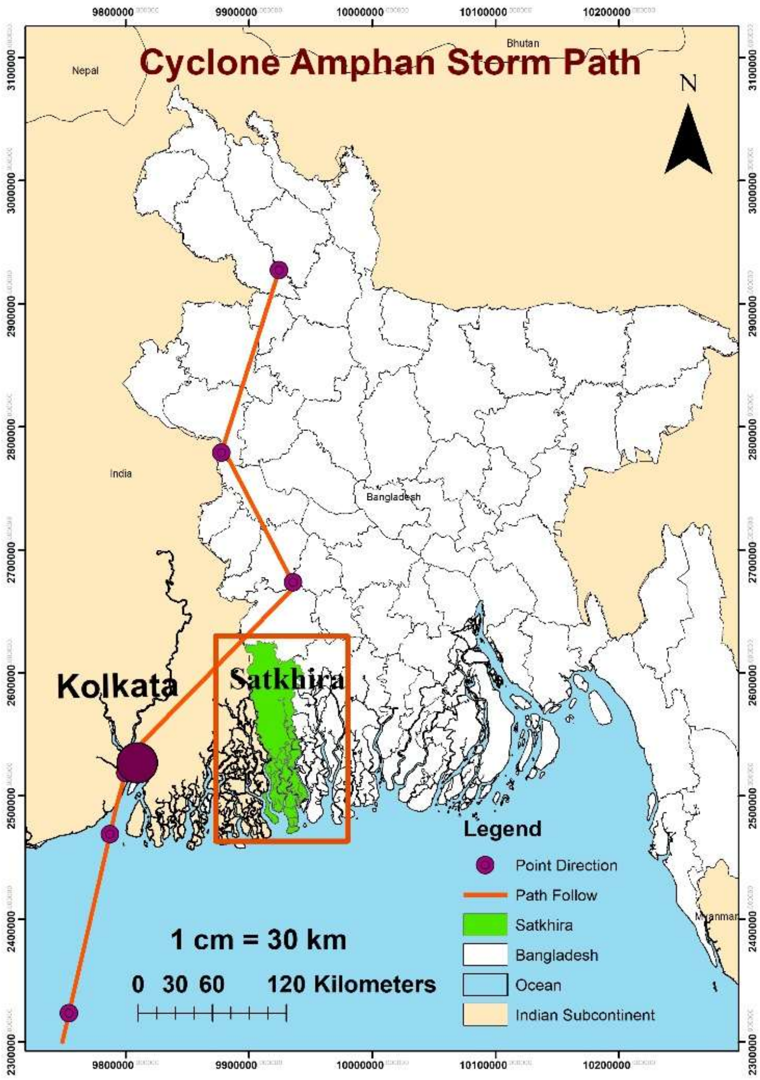

Figure 2. Cyclone Amphan path associated with study area, Satkhira district under Khulna Division in Bangladesh. Cyclone path follows most of the southwestern part of Bangladesh associated with Kolkata, India.

DOI10.5595/001c.123359

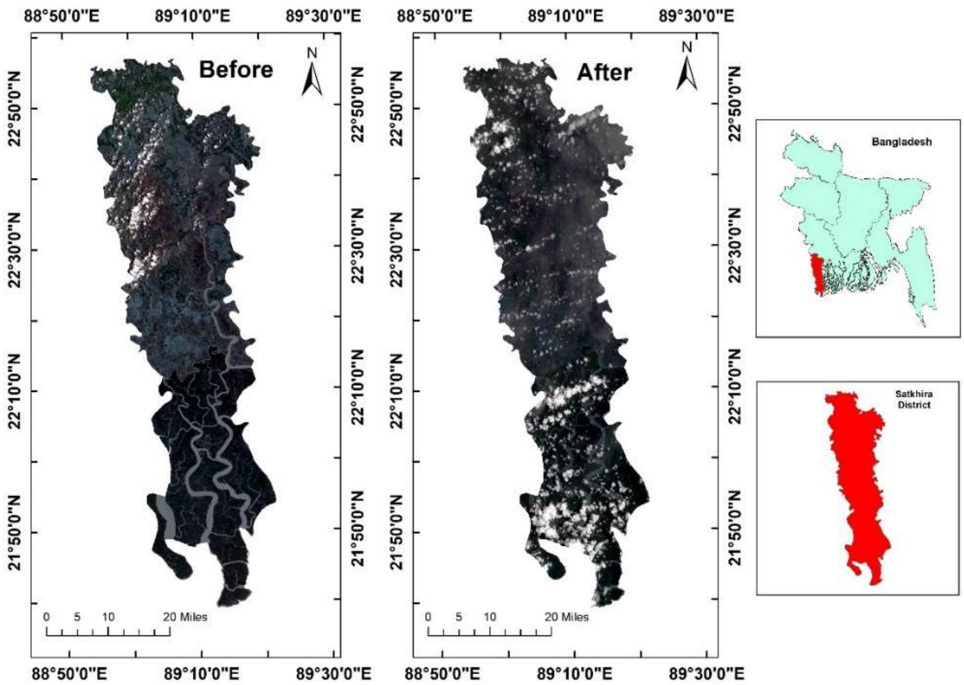

Figure 3. Acquired Landsat-8 satellite images before (May 08, 2020) and after (June 09, 2020) the Cyclone Amphan in the study area with clouds in white color.

2.2 Pre-processing and Correction of the Input Data Headings

The pre-processing of satellite data always helps extract information from satellite imagery (Islam et al., 2018). ArcGIS software is used to perform the processing of the images. Bands 2,3,4 and 8 of Landsat-8 were stacked and converted into a single layer with the help of a layer stacking tool. Using the shapefile of the study area, AOI has been created and masked by a subset tool. The geographic coordinate system of the satellite images was World Geodetic System (WGS) 84, and the projected coordinate system was Universal Transverse Mercator (UTM) Zone 45N. The acquired image data were radiometrically and geometrically corrected required.

2.3 Image Classification

Iso-cluster unsupervised classification tool has been used to classify Landsat-8 satellite imagery of pre and post cyclone Amphan of the study region. Six different land cover types were selected to identify distinct land cover features. The classes are (1) Water Body, (2) Vegetation, (3) Agricultural land, (4) Barren land, (5) Low land and (6) Urban area (Table 2) described the land use categories that are used to define land use classes.

DOI10.5595/001c.123359

Table 1. Comprehensive data about the satellite images applied in this work. Pre- and post-cyclone satellite imageries were applied for assessing the damage in the study areas.

Satellite ID	**Sensor ID**	**Path / Row**	**Date of Acquisition**	**Spatial Resolution (m)**	**Bands (µm) (Using bands for layerstack)**	**Data Source**
Landsat -8	OLI/ TIRS	138/44 138/45	**08/05/2020**	30	B2 (Blue) :0.45–0.51 B3 (Green):0.53-0.59 B4 (Red) : 0.64–0.67 B5 (NIR) : 0.85–0.88 B8 (Panchromatic): 0.50-0.68	USGS Landsat Collection 1 Level-1 & NASA-GLCF
Landsat -8	OLI/ TIRS	138/44 138/45	**09/06/2020**	30	B2 (Blue) :0.45–0.51 B3 (Green):0.53-0.59 B4 (Red) : 0.64–0.67 B5 (NIR) : 0.85–0.88 B8 (Panchromatic): 0.50-0.68	

Table 2. Land use and land cover classification pattern applied in the pre and post-cyclone satellite images.

Land use / Land cover types	Features
Water body	Rivers, Ponds, Lakes, Lagoons and Fishing areas
Vegetation	Dwelling vegetations, mangroves, Shrubs & Bushes
Agricultural land	Land devoted to agriculture, permanent crops, such as fruits, vegetables & others cultivable areas
Barren land	Non-urban settings, riverbank, barren lands, landfills, dune, bare soils & sandy beaches
Low land	Riverbank, Deposited lands & Accreted lands
Urban area	Built-up area including industrials, commercials, residential and other infrastructures

A base map was prepared with the help of Google Earth Pro. This was crucial to categorize the land cover classes more precisely. The area, A (in km^2), of each class calculated from the attribute table by using the following formula:

$$A = \frac{Cellsize * Count}{10^6} \tag{1}$$

Normalized Difference Vegetation Index (NDVI) is also performed in the study area, which allows us to determine the greenness of vegetation over regional to global scale and the changes in vegetation growth rate (Salman et al., 2021; Gandhi et al., 2015). Multispectral satellite data acquired from Landsat-8 are used for NDVI classification. Theoretically, the NDVI value ranges from -1.0 to 1.0. Nevertheless, for the earth surface, the value range of NDVI is -1.0 to 0.7 (Suzuki et al., 2000). The NDVI can be expressed as follows:

$$NDVI = \frac{NIR-RED}{NIR+RED} \tag{2}$$

2.4 Accuracy Assessment Calculation

Accuracy assessment is prime important for pre- and post-classified images. Likewise, the Kappa coefficient values between 0.61-0.80 represent the substantial agreement (Landis & Koch, 1977). In this study, user, producer and overall as well as Kappa coefficient, are calculated through the following equations:

Overall Accuracy (OA):

$$OA = \frac{N_D}{N} \times 100 \tag{3}$$

Where, N_D is the total number of correctly classified pixels (diagonal) and N is Total Number of Reference Pixels.

User Accuracy (UA):

$$UA = \frac{N_C}{R_N} \times 100 \quad (4)$$

Where, N_C equivalences to number of correctly classified pixels in each category and on the other side, R_N is the total number of classified pixels in that category (The Row Total).

Producer Accuracy (PA):

$$PA = \frac{N_C}{C_N} \times 100 \quad (5)$$

Where, N_C equivalences to number of correctly classified pixels in each category and on the other side, C_N is the total number of classified pixels in that category (The column Total).

Kappa Coefficient (T):

$$T = \frac{(\boldsymbol{TS} \times \boldsymbol{TCS}) - \sum \text{(Column Total} \times \text{Row Total)}}{\boldsymbol{TS}^2 - \sum \text{(Column Total} \times \text{Row Total)}} \times 100 \quad (6)$$

Where, TS means the total number of samples taken, and TCS is the total number of correct samples.

2.5 Change Detection

The changes in the land cover between pre- and post-cyclone Amphan are determined with the post-classification comparison change detection algorithm. Dewan and Yamaguchi (2009) use a post-classification algorithm for tropical cyclone impact assessment. The analysis procedure was performed by following the underlying flowchart (Figure 4).

3. RESULT AND ANALYSIS

3.1 Unsupervised Images Classification

An overall of 3593.62 km^2 of the land region was assessed for the Satkhira district after unsupervised image classification using ArcGIS (Figure 5).

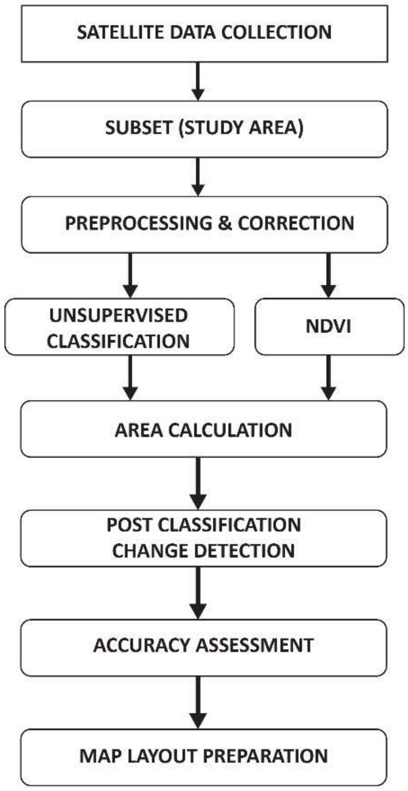

Figure 4. A workflow approach in the context of the present study.

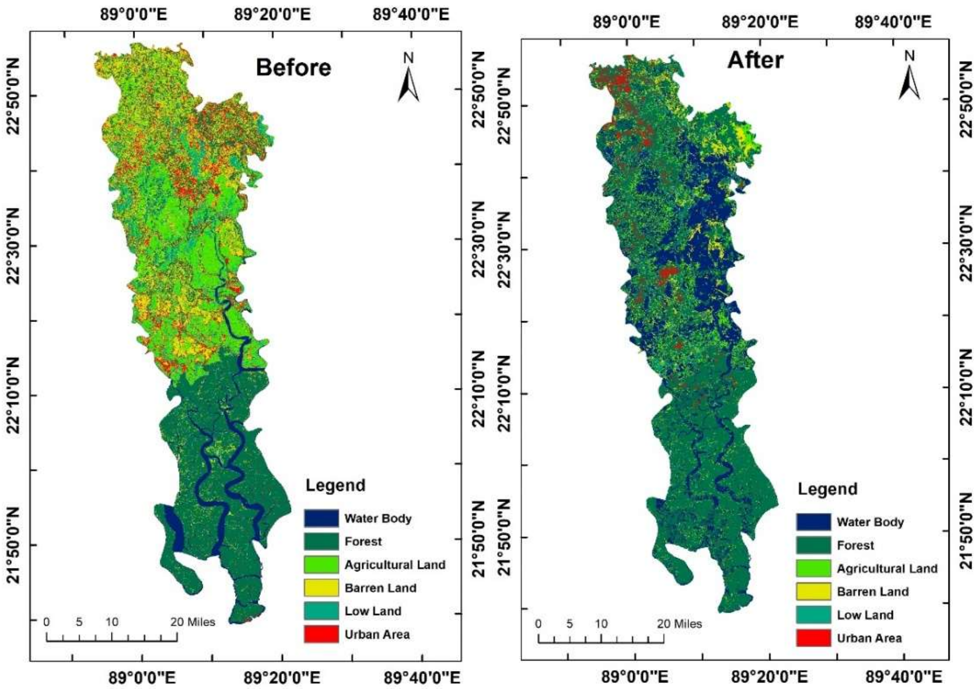

Figure 5. Portion of the study area site representing pre- and post-cyclone images acquired on 8th May, 2020 and 9th June, 2020 respectively with the used unsupervised Classification schemes. Results signify that the entire areas were covered by storm waters due to Cyclone Amphan.

3.2 Accuracy Assessment

In remotely sensed data, the assessment of accuracy is vital to assess the heterogeneity and proof of the classified imageries (Elkington, 1987). The pre and post cyclone classified imageries were accurately assessed with high-resolution Google Earth imageries of the studied region. Thirty ground control points have been taken for each class. The water bodies can be easily identified from Google Earth; however, other classes were difficult to distinguish. Especially the agricultural land and barren land are mostly similar. The complete accuracies for pre and post cyclone classification were 70% and 68.33%, respectively. Kappa accuracy was obtained at 0.64 for pre cyclone and 0.62 for post cyclone classification, and it can be concluded that our unsupervised classification has a considerable agreement consequently Landis and Koch (1977).

3.3 Damage Analysis

Comparing the pre and post cyclone image classification gives us information about the cyclone impact on the study region. It was anticipated that the land cover classes' changed within 30 days in the study area due to cyclone Amphan. Statistical analysis between two classified images strongly supports this assumption. It indicates that most of the area is highly or partially damaged by analyzing the results due to the vulnerability of cyclone Amphan. Major changes can be seen in the water body flooded or storm water in the study area. Before the cyclone Amphan, the total water body shared 407.42 km^2 (11.34%), and after the tropical cyclone, the water body covered 1038.31 km^2 (28.89%) of the total study area because of storm water effects (see Figures. 6,7 and Table 3). Changes in vegetation are also interpreted from the classified image. The biggest mangrove forest, Sundarban, is situated in the southern part of the Satkhira district. Before the cyclone, the area enclosed with vegetation was 1865.72 km^2 (51.92%), and after the catastrophic cyclone, the vegetation shared 1717.31 km^2 (47.79%) in the study area (Figure 6 and Table 3).

The cyclone dramatically affected the agricultural land changing the area from 686.72 km^2 (19.11%) to 297.5 km^2 (8.29%) (Figure 6,7 and Table 3). Most of the agricultural land has been gone underwater due to heavy flashes during the cyclone. Crops in the field were heavily damaged. In the study area, the barren land and the low land were also affected by the cyclone. The change in their area before and after the cyclone is quantified from the classified image. Before the cyclone, the barren land was calculated, which was 303 km^2 (8.43%), and after the cyclone, it shared 238.25 km^2 (6.63%) (Figure 6,7 and Table 3). Due to the strong surge of water, the closed water bodies increased dramatically in different land cover areas. Low land areas were also flooded due to heavy flashes of water, and the damage can be seen by looking into the statistical analysis. It changed from 203.81 km^2 (5.67%) to 190.81 km^2 (5.31%) (Figure 6,7 and Table 3). A relative change in the urban area can be seen between two classified images. Tropical cyclones largely affect human lives and properties, and there was no exception for the cyclone Amphan. Changes in urban areas from 126.95 km^2 (3.53%) to 111.44 km^2 (3.10%) were also quantified from the classified image (Figure 6,7 and Table 3).

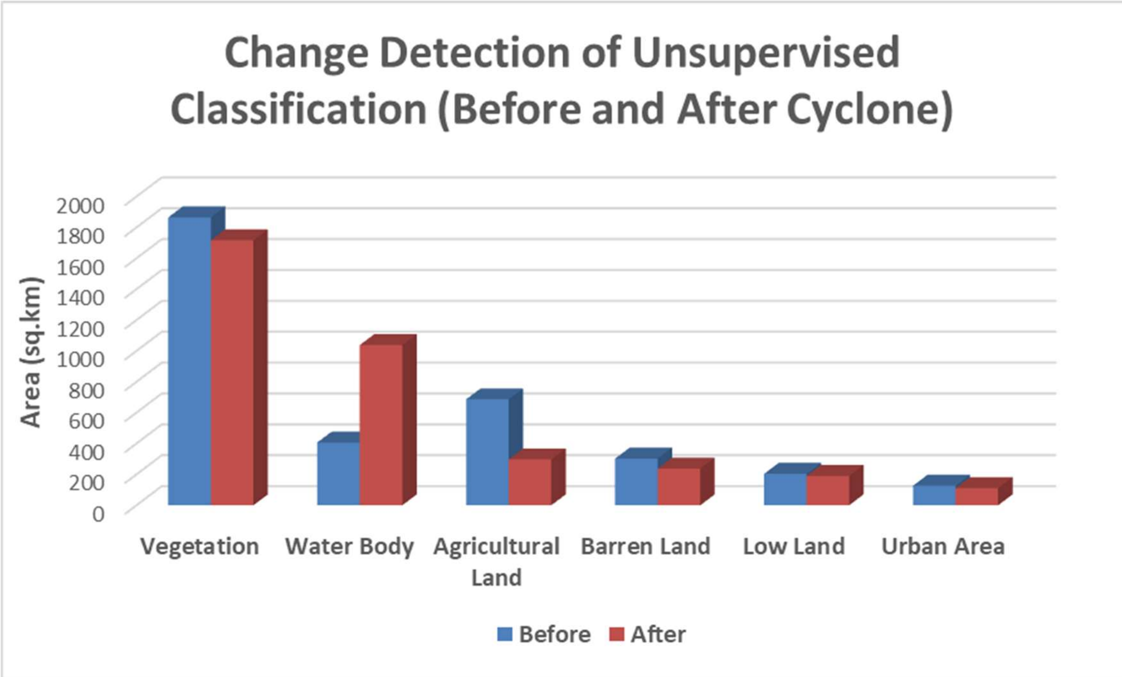

Figure 6. The alteration of land cover affected by tropical cyclone Amphan in the studied region. Results reveal that all the land use/land cover componets were declined whereas water bodies were increased.

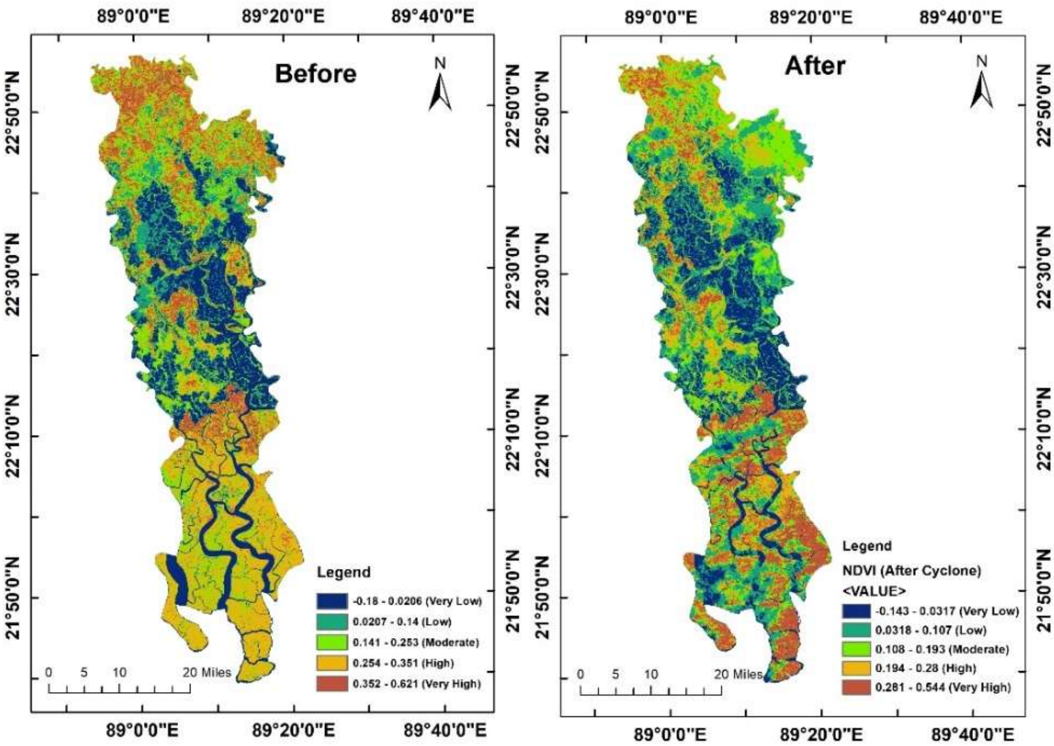

Figure 7. Portion of the study area site representing pre and post cyclone images acquired on 8th May, 2020 and 9th June, 2020 respectively with the used NDVI analysis schemes.

3.4 NDVI Analysis

The NDVI images of before and after cyclone assessed the degree of impact brought about by cyclone Amphan in the study area. Different pixel values identify the changes. For example, the highest NDVI value is decreased significantly after the cyclone in contrast to the before. Before the cyclone, the NDVI image displays very high pixel value (0.352-0.621) in the southern part, where the Sundarbans mangrove forest is located (Figure 8). High vegetation is identified with this value in this area. After the cyclone, the range of the highest NDVI value (0.281-0.544) is decreased, which indicates that the cyclone Amphan created havoc in many parts of the Sundarbans (Figure 7). The vegetation health of the study region deteriorates from pre to post cyclone, which shows the actual damage. The NDVI value in the eastern part decreases between two periods. The lowest value in NDVI mainly represents water. Because of waterlogging in many areas, the lowest value increases in many portions of the study region. In the eastern part, the NDVI ranges -0.18-0.021 in the pre-period and -0.143-0.032 in the post-cyclone period. The decreasing value of moderate NDVI is also seen in the western area for a particular NDVI range. The moderate value range of 0.141-0.253 in pre-cyclone data is covered with a lower value in post-cyclone (0.108-0.193). Comparing the pre- and post-cyclone NDVI data results, it can conclude that there is no destruction of any vegetation species, but the vegetation damage is significant.

Table 3. Category wise land use and land cover distribution of Satkhira (before and after cyclone Amphan). Overall, findings show that agricultural, vegetation, barren and low lands were covered by storm surge water and water logging due to cyclone Amphan.

	Land use Category	**Land use (A) Pre Cyclone Area (km^2)**	**% of Land**	**Land use (B) Post Cyclone Area (km^2)**	**% of Land**
1	Water Body	407.42	11.34	1038.31	28.89
2	Vegetation	1865.72	51.92	1717.31	47.79
3	Agriculture	686.72	19.11	297.5	8.29
4	Barren land	303	8.43	238.25	6.63
5	Lowland	203.81	5.67	190.81	5.31
6	Urban area	126.95	3.53	111.44	3.10
	Total	**3593.62**	**100**	**3593.62**	**100**

4. CONCLUSIONS

The study makes an attempt to assess the potential damage and loss of the Bangladesh's top rated devastating region, Satkhira district, to a harshly cyclone Amphan, which was desolated the region on 20 May, 2020. There is a research gap between damage and loses assessment of the studied regions to extraordinary events like cyclone in the literature, which analysis longing to complete. Such studies may assume an intense work in forming the improvements of the regions for the Government and NGOs authorities. The study verified the potentiality of a technological approach of remote sensing for evaluating manifold damages caused by the cyclone Amphan utilizing an object based unsupervised technique from Landsat-8 imageries. In precise, 30 m spatial resolution Landsat-8 imageries were fit for representing pre- and post-cyclone land-use/land cover in the studied region with a high level of accuracy and specified the practicality of an object based tactic in this study.

A contrast between the pre and post cyclone image classification gives us evidence about the cyclone impact on the study area. Statistical analysis indicates that most of the area is highly or partially damaged by analyzing the results due to the vulnerability of cyclone Amphan. Inundated water body flooded or storm water in the study area has increased from 11.34% to 28.89%. In contrast to the water body, the vegetation decreased from 51.92% to 47.79% of the classified image. The impact of the cyclone dramatically affected agricultural land, reducing their area from 19.11% to 8.29% of the entire study region. Similar to farming land, the barren land decreased from 8.43% to 6.63% after the cyclone. Low land areas were also flooded due to heavy flashes of water, and it changed from 5.67% to 5.31%. Changes in urban areas were also quantified from 3.53% to 3.10% by the classified images.

The NDVI analysis of pre and post cyclone measured the degree of impact brought about by cyclone Amphan in the study region. The highest value of NDVI is decreased significantly after the cyclone in contrast to the before. Therefore, comparing the pre- and post-cyclone NDVI data results, it can be concluded that there is no demolition of any vegetation species, but the vegetation damage is substantial. Further measurement could likewise scrutinize and follow the restoration of the study areas from such contemptible events. Eventually, comparable vulnerability and capability assessment, mapping of the other potential unpleasant areas in Bangladesh can sustain the communal authority outspread its policies and foundations.

ACKNOWLEDGEMENTS

The value of this manuscript draft is considerably enhanced from the remarks and recommendations of three anonymous critics. The authors express thankfulness towards them for their remarks. In addition, the authors are indebted to the experts of USGS. The study is possible due to the free imagery provided by them.

REFERENCES

Balasubramanian S., and Chalamalla V. K. (2020). Super Cyclone Amphan: A Dynamical Case Study. 1–10. http://arxiv.org/abs/2007.02982

Das P. K. (1972). Prediction model for storm surges in the Bay of Bengal. *Nature*, *239*(5369), 211–213. https://doi.org/10.1038/239211a0

Dewan A. M., and Yamaguchi Y. (2009). Land use and land cover change in Greater Dhaka, Bangladesh: Using remote sensing to promote sustainable urbanization. *Applied Geography*, *29*(3), 390–401. https://doi.org/10.1016/j.apgeog.2008.12.005

Didar-Ul Islam S. M., Bhuiyan M. A. H., and Ramanathan A. L. (2015). Climate Change Impacts and Vulnerability Assessment in Coastal Region of Bangladesh: A Case Study on Shyamnagar Upazila of Satkhira District. *Journal of Climate Change*, *1*, 37–45. https://doi.org/10.3233/JCC-150003

Elkington M. D. (1987). A review of: "Remote Sensing Digital Image Analysis: An Introduction". By J. A. Richards. (Berlin, Heidelberg. New York: Springer-Verlag, 1986.) [Pp. 281] Price DM 138. *International Journal of Remote Sensing*, *8*(7), 1075. https://doi.org/10.1080/01431168708954750

FLIERL G. R., and ROBINSON A. R. (1972). Deadly Surges in the Bay of Bengal: Dynamics and Storm-tide Tables. *Nature*, *239*(5369), 213–215. https://doi.org/10.1038/239213a0

Gandhi G. M., Parthiban S., Thummalu N., and Christy A. (2015). Ndvi: Vegetation Change Detection Using Remote Sensing and Gis - A Case Study of Vellore District. *Procedia Computer Science*, *57*, 1199–1210. https://doi.org/10.1016/j.procs.2015.07.415

Henderson-Sellers A., Zhang H., Berz G., Emanuel K., Gray W., Landsea C., Holland G., Lighthill J., Shieh S. L., Webster P., and McGuffie K. (1998). Tropical Cyclones and Global Climate Change: A Post-IPCC Assessment. *Bulletin of the American Meteorological Society*, *79*(1), 19–38. https://doi.org/10.1175/1520-0477(1998)079<0019:TCAGCC>2.0.CO;2

Hoque M. A., Phinn S., Roelfsema C., Childs I. (2016). ASSESSING TROPICAL CYCLONE DAMAGE USING MODERATE SPATIAL RESOLUTION SATELLITE IMAGERY:CYCLONE SIDR, BANGLADESH 2007, Proceedings of the 36th Asian Conference on Remote Sensing 2015.

Islam K., Jashimuddin M., Nath B., Nath T. K. (2018). Land use classification and change detection by using multi-temporal remotely sensed imagery: The case of Chunati wildlife sanctuary, Bangladesh. *Egyptian Journal of Remote Sensing and Space Science*, *21*(1), 37–47. https://doi.org/10.1016/j.ejrs.2016.12.005

Klemas V. V. (2009). The role of remote sensing in predicting and determining coastal storm impacts. *Journal of Coastal Research*, *25*(6), 1264–1275. https://doi.org/10.2112/08-1146.1

Knutson T. R., McBride J. L., Chan J., Emanuel K., Holland G., Landsea C., Held I., Kossin J. P., Srivastava A. K., Sugi M. (2010). Tropical cyclones and climate change. *Nature Geoscience*, *3*(3), 157–163. https://doi.org/10.1038/ngeo779

Landis J. R., Koch G. G. (1977). Landis amd Koch1977_agreement of categorical data. *Biometrics*, *33*(1), 159–174.

Murty T. S., Flather R. A., Henry R. F. (1986). The storm surge problem in the bay of Bengal. *Progress in Oceanography*, *16*(4), 195–233.

https://doi.org/https://doi.org/10.1016/0079-6611(86)90039-X

Salman M.A., Nomaan M.S.S., Sayed S., Saha A., Rafiq M.R. (2021). LAND USE AND LAND COVER CHANGE DETECTION BY USING REMOTE SENSING AND GIS TECHNOLOGY IN BARISHAL DISTRICT, BANGLADESH. Earth Sciences Malaysia (ESMY). DOI: http://doi.org/10.26480/esmy.01.2021.33.40

Salman M.A., Hasan S.M.R, Ahmed S., Tahsin M., Khan N. (2018). Shoreline Change Rate along the Southern Coast of Bangladesh due to Climate Change using Remote Sensing & ArcGIS Technology. IJETAE.

Salman M.A., and Ahmed F. (2020). Climatology In Barishal, Bangladesh: A Historical Analysis Of Temperature, Rainfall, Wind Speed And Relative Humidity Data. DOI: 10.26480/mjg.01.2020.43.53

Salman M.A. (2022). Assessment of vulnerability and capacity to the cyclone 'Amphan' impacts of the southwestern coastal part of Bangladesh: an empirical contextual investigation. *Natural Hazards*, *15*, 1715–1742. https://doi.org/10.1007/s11069-022-05615-1

Suzuki R., Tanaka S., Yasunari T. (2000). Relationships between meridional profiles of satellite-derived vegetation index (NDVI) and climate over Siberia. *International Journal of Climatology*, *20*(9), 955–967. https://doi.org/10.1002/1097-0088(200007)20:9<955::AID-JOC512>3.0.CO;2-1

Vatsavai R., Tuttle M., Bhaduri B., Bright E., Cheriyadat A., Chandola V., Graesser J. (2011, July 24-29). *Rapid damage assessment using high-resolution remote sensing imagery: Tools and techniques*[Conference session]. 2011 IEEE International Geoscience and Remote Sensing Symposium. Vancouver, BC, Canada. https://doi.org/10.1109/IGARSS.2011.6049338